INVITED PAPERS

The Appearance and Origin of Common Magnetic Resonance Imaging Artifacts, and Solutions for Alleviating Their Effects

Puneet S. Sharma, PhD[1] and John N. Oshinski, PhD [1,2].

[1] Department of Radiology and Imaging Sciences, Emory University School of Medicine, 1364 Clifton Road, Atlanta GA 30322
[2] Department of Biomedical Engineering, Emory University School of Medicine, 1364 Clifton Road, Atlanta GA 30322

Abstract – The appearance of image artifacts in magnetic resonance imaging (MRI) continues to be an area of confusion for many medical physicists. Much of the complexity in the appearance of artifacts comes from the fact that image data is acquired in frequency-phase space (k-space) and the artifacts' appearance is related to how the signal is transformed into image space. Here we give a brief non-mathematical explanation of the elements of image quality and image acquisition, and present many of the most common image artifacts in the context of this explanation. Solutions for eliminating or mitigating the effects of these artifacts are offered.

Keywords – MRI, Magnetic Resonance Imaging, Artifacts, Physics

1. Introduction

One of the pervasive truths about Magnetic Resonance Imaging (MRI) is that all acquisitions possess some degree of image artifacts. An image artifact is any feature that is present in an image that is not present in the original object. Sometimes artifacts are severe enough to obscure diagnostic interpretation or cause a mis-diagnosis, while others are insignificant or imperceptible to the radiologist. The medical physicist must be able to recognize artifacts and understand why they occur. Furthermore, it is important to outline possible remedies for more deleterious artifacts, and what personnel are most equipped to solve them (technologist, physicist, or vendor service engineer). MRI artifacts are generally classified into three broad groups: 1) Physiological-related, 2) System- or parameter-related, 3) Reconstruction-related.

Physiological artifacts evolve from the interaction between the subject and the MR system during acquisition. Specifically, it is important to understand how the MR pulse sequence is affected by the anatomy and physiology of interest. System-related artifacts stem from degradation or transient effects in the MR system and/or acquisition components. Establishing a local quality assurance (QA) program and periodic vendor-led preventative maintenance (PM) help recognize and ameliorate these issues. Reconstruction artifacts result from non-optimal implementation or failure of the reconstruction algorithm, such as artifacts arising from parallel imaging reconstruction.

In this article, we will outline the most common MR artifacts, including details about their mechanism, and we provide suggestions for possible solutions. We will pay special attention to pulse sequences and system configurations most usually affected by these artifacts. In addition, we will discuss aspects of a quality assurance program, especially the role of the MR Physicist in clinical practice. It is important to begin the discussion of artifacts by first considering the elements that constitute high quality MRI, followed by a brief review of k-space signal acquisition principles, then presentation and characterization of the artifacts.

1.2 ELEMENTS OF OPTIMAL MR IMAGE QUALITY

At its core, the goal of any modality and image acquisition strategy is to produce diagnostic information with consistently high image quality. Though this concept is abstract, high image quality can be defined empirically as possessing high signal- and contrast-to-noise, high resolution, and minimal artifacts, while achieving scan times as low as possible. This pursuit, however, is tempered by a variety of tradeoffs. In MRI, fast-imaging generally comes at the expense of each of these image characteristics, but primarily image resolution and signal-to-noise. Consider the basic equation for MR scan time (for 3D imaging) (1) :

$$Scan\ time = TR \times N_y \times N_z \times NSA \qquad [1]$$

Where TR is the sequence repetition time, N_y and N_z are the number of y- and z-phase encode steps, respectively, and NSA is the number of signal averages. It can be seen immediately that scan time is proportional to phase resolution (N_y and N_z) and signal strength (NSA), with repetition time largely dictated by the desired contrast of the image acquisition. There are more detailed parameters in an MRI acquisition that affect Equation 1, such as image matrix, slice thickness, slices, and bandwidth. These other parameters are typically defined by the requisite anatomical coverage, contrast sensitivity, and image resolution criteria set forth by radiologists and physicians based on specific needs for disease characterization. Though disease contrast resolution is of utmost importance in diagnostic MRI, the basic relationship that ultimately governs image quality is signal-to-noise ratio (SNR). MRI signal is proportional to the amount (and strength) of the magnetization in a voxel, and signal averaging. Measured noise, however, is proportional primarily to the acquisition readout bandwidth (BW_{read}), assuming other thermal and resistive components are relatively invariable. Hence the SNR per voxel (for 3D imaging) is:

$$SNR \propto K \cdot (\Delta x \cdot \Delta y \cdot \Delta z) \cdot \left(\sqrt{\frac{NSA \cdot N_x \cdot N_y \cdot N_z}{BW_{read}}} \right)$$

Where K represents all other imaging factors (coil, field strength, relaxation, tissue parameters, etc). The form of Equation 2 can be rewritten to describe relationships with other parameters, such as field-of-view (FOV), by substituting known equivalencies (i.e. $\Delta x = FOV/N_x$). This is beneficial when considering the consequences of fixed variables (such as Δx) on SNR (1).

The overlap between Equation 1 and 2 is clear, and one begins to understand the tradeoff among resolution, SNR, and scan time, especially the cost of high resolution imaging. For instance, if resolution N_y is doubled, SNR reduces by $1/\sqrt{2}$, while scan time is doubled. It is important to consider these costs quantitatively, but only in light of baseline SNR and scan time values. One may also choose to normalize SNR against scan time for better describing scan efficiency.

The complete picture of high MR image quality must also integrate equipment variables, contrast mechanisms, and imaging artifacts. While the former two elements can be gauged as part of preventative maintenance and disease-driven protocol criteria, respectively, and absorbed by the "K" term of Equation 2, image artifacts are primarily monitored and assessed qualitatively. In the sections to follow, we will investigate where and when artifacts present themselves, while later presenting methods to help track and resolve artifacts programmatically.

1.2. K-SPACE PRINCIPLES

The three broad MR artifact categories outlined earlier (System, Reconstruction, and Physiologic) have effects on MR image acquisition that cause it deviate from the ideal scenario. MRI uses rapidly switching linear magnetic field gradients to specifically encode the origin of measured signal repeatedly over the duration of an acquisition. These gradients cause the image data to be acquired in frequency-phase space (or k-space), and therefore a significant emphasis is placed on the integrity of the raw (or k-space) data. As unwanted intrinsic and extrinsic factors alter the specific encoding and signal acquisition process, the measurement of MR data becomes discordant with expected phase- and frequency-encoded values. Whether raw data is collected all-together in one-TR, or periodically over multiple TRs, the relationship between the multiple encoded signals in k-space, and when they were temporally acquired, play an important role in predicting the prevalence of MR artifacts. For this reason, it is important to briefly discuss the key principles of 2D Fourier imaging and k-space.

In order to generate a grey-value for every voxel in the image, a method must be applied to spatially localize the spin density. The most widely used method is 2D Fourier imaging whereby applying a linear magnetic field gradient in one direction (e.g. x-direction) causes the Larmor frequency of the excited spin density to vary predictably across the field-of-view. The resultant (echo) signal (produced by either gradient or spin echo) is therefore regarded to be a combination of defined spatial-frequencies. The notion that a linear gradient provides a spatial- and time-dependent change in the precession frequency (and phase) of the spin density allows convenient interpretation using well-studied Fourier analysis. For the second dimension (i.e. y-direction), further frequency-encoding cannot be applied since unique assignment of spatial-frequency will not be possible for all unknown voxels. To overcome this, a brief linear gradient "pulse" is applied in the y-direction prior to frequency encoding. The consequence of a finite gradient is to impart a specific phase-shift along the second-dimension. To provide enough unique data to satisfy Fourier analysis and recover the original spin density, the process of phase-encoding is repeated every TR (or echo-signal), with the gradient amplitude incremented (ΔG_y) each time and followed by frequency encoding during data collection.

Since the individual ΔG_y step size and duration (τ_y) is known, the frequency-encoded echo signal can be measured and recorded into a particular "address" in k-space. The raw data points in k-space are discrete due to signal digitization, and therefore assigned k_y and k_x indices related by the equations:

$$k_x = \gamma G_x \Delta t$$
$$k_y = \gamma \Delta G_y \tau_y$$

In essence, each point in k-space (k_x, k_y) represents a spatial frequency, or oscillation "pattern". The intensity of the point signifies the weighted contribution of the frequency pattern to the original image features. The center of k-space represents low frequency patterns and, thus, the

majority of overall signal strength of the image. The periphery of k-space represents high frequency components, which more define the sharp signal changes in the image, such as near tissue interfaces and edges. Since the discrete Fourier transform connects the raw k-space data to image space, reconstruction is subject to transform properties, and artifacts in the acquired raw frequency-phase data transformed into the image data (1).

2.0. REVIEW OF MRI ARTIFACTS

The concepts of k-space acquisition and Fourier transform properties provide the medical physicist the background to understand the role of the MR acquisition process in the generation and appearance of image artifacts. However, the diagnosis of MR artifacts begins at the image level by recognizing distinct abnormalities in the image. It is important to distinguish image artifacts from poor signal-to-noise ratio or poor contrast-resolution, which are generally overcome through protocol optimization (although some poor SNR may be system- or electronics-related). In the sections to follow, we will describe the appearance and origin of commonly encountered artifacts, highlighting their sensitivity to system and reconstruction imperfections, patient physiology, and suggest solutions for mitigating or alleviating artifacts.

2.1. PHYSIOLOGIC ARTIFACTS: MOTION AND PHASE ENCODING EFFECTS

Appearance: Physiologic motion causes image artifacts, the most prevalent being image ghosting, *figure 1*. The "ghost" terminology originates from the observation of faint replicated copies of the imaged structures along the phase encode direction. Image ghosts may also be very distinct, especially if the moving object is high signal, such as fat or fluid. The occurrence of this artifact is a result of k-space sampling during the motion of an imaged object. In clinical practice, this is mostly caused by patient movement, breathing, blood flow, or cardiac motion. Even subtle motion, such as eye movement and swallowing, can cause motion-related ghosting.

Origins/Causes: The propagation of ghosts along the phase encode direction distinguishes them from other similar artifacts, such as truncation (or Gibbs "ringing") artifacts, which occur in all directions, and will be discussed later. The sensitivity to the phase encode direction evolves from the relatively slow sampling rate of phase encode steps relative to the motion of a moving object. The effective sampling rate in the phase encode direction is on the order of 1 to 100Hz (1/TR, for single-echo imaging), compared to kHz ($1/\Delta t = BW_{read}$) in the frequency encode direction. Therefore, during periodic motion, such as breathing in abdominal imaging, each phase step may encode information from a different diaphragm position over the course of an MR acquisition. This measurement inconsistency among the phase encode steps has two main consequences: 1) the absolute signal strength (due to inflow, tissue spin density, etc.) may vary between steps and 2) an additional phase shift is accrued due to tissue positional changes. Since MRI acquisitions assume the signal changes exclusively from k-space localization, this inconsistency causes k-space variability in the phase encode direction. This phase and signal variability is dependent on the sampling rate and the periodicity (and intensity) of the object motion.

Location: The properties of Fourier transform, which result from phase shifts in k-space due to *periodic* motion, cause a corresponding position shift of the object in the reconstructed image, resulting in ghosts. The degree of spatial shift is proportional to the displacement of the motion, so small motion results in ghosts with small displacements from the object. For *non-periodic* motion, the presentation of motion ghosts in images may appear somewhat random, especially if motion contains several harmonics, such as irregular breathing, eye-blinking, or gross head movements. In these cases, distinct ghosts are often not visualized, but rather blurring in the phase encoding direction predominates. If motion is fast enough, ghosts or blurring may also occur in the frequency encode direction. However, ghosting predominantly occurs due to motion is typically in the phase encoding direction.

Strategies for Alleviating Artifacts: Several methods are available to compensate for motion artifacts. A simple method is to swap the phase- and frequency-encode direction. Though not eliminated, this tactic can redirect motion ghosts into other directions, thereby revealing relevant anatomy. This performs best for small-dimensioned ghosts, such as those from vessels, eye-movement, swallowing, and peristalsis.

Since the variability of additional phase shifts in k-space dictate the occurrence of ghosts in the final image, synchronizing phase encode steps with motion eliminates inconsistencies. In the common case of respiration, this is accomplished through respiratory or navigator gating, in which a breathing belt or additional 1-D MR data across the diaphragm enables real-time tracking of abdominal and diaphragm movement. This system is configured to accept or discard raw data based on respiratory position, such as end-expiration. Though effective, respiratory gating has noteworthy shortcomings: 1) accepting only consistent data may result in lengthy scan times; and 2) an often integrated "data acceptance window" (+/- 2mm) may re-introduce some minor phase shifts, causing some subtle ghosts in the final image. When possible, routine abdominal imaging relies on breath hold imaging. However, its effectiveness clearly depends on patient cooperation, and fast imaging techniques optimized for quality and scan time. Modern MR systems are increasingly capable of high resolution breath hold imaging through advanced acceleration techniques, such as parallel imaging (2,3) and compressed sensing (2).

Data averaging is another method to reduce motion-induced ghosts. This is achieved by increasing the number

of signal averages (NSA), which also invariably increases scan time. MR signal averaging re-acquires each phase encode step, which is then combined to previous data prior to reconstruction. Essentially, data averaging reduces the degree of k-space variability by making phase transitions more gradual. While distinct phase ghosts can be eliminated, the result is more image blurring. The degree of effectiveness of this solution depends on the clinical application. Diffusion-weighted imaging (DWI) of the abdomen benefits from signal averaging since the subtle edge-blurring of large coherent tissue motion does not affect the small incoherent diffusion motion encoding imposed by the large diffusion-sensitizing gradients (4). Moreover, DWI is often acquired using a "single-shot" echo-planar (EPI) technique, which collects all phase-encode steps sequentially in less than 300ms. This pulse sequence strategy is itself motion-insensitive, since the k_y sampling frequency is significantly increased, effectively "freezing" bulk tissue motion. Single-shot MRI has also become routine for T2-weighted abdominal imaging. Some drawbacks persist, such as edge blurring, due to signal decay over the echo-train, and slice mis-registration for multi-slice acquisitions.

Another method to compensate for motion artifacts is to acquire k-space data with a radial trajectory. A radial trajectory through k-space is achieved by performing gradient frequency encoding in both the k_x and k_y directions, simultaneously. Similar to "single-shot" approaches, this allows the k-space sampling rate in each direction to be on the same order (kHz) during one TR. In addition to sampling k-space at a fast rate compared to object motion, the trajectory also passes though the center of k-space every TR period. This has a similar effect as signal averaging, since similar central k-space samples are acquired repeatedly, albeit at a higher rate. The amount of low k-space oversampling density is directly proportional to motion artifact reduction. However, a disadvantage is that high k-space data has subsequently lower sampling density, which introduces new artifacts, such as streaking. To achieve high motion-insensitive quality with radial k-space, lengthy scan times are often needed to provide sufficient sampling density.

3.0. SYSTEM-RELATED ARTIFACTS

3.1. NYQUIST GHOSTING

Appearance: Similar to motion, Nyquist ghosting are artifacts appear as distinct copies of the imaged object, propagated across the FOV in the phase encode direction, *figure 2*. The Nyquist ghost is often referred to as "N/2" ghosts, since the object is shifted half (N/2) the FOV in the phase encode direction. However, the object shift could be less (e.g N/8, etc) if the data acquisition is divided into more segments (e.g 4 segments). The effect is mainly seen with echo-planar imaging (EPI) or partial Fourier imaging, which requires rapid gradient switching to capture complete k-space data within a short duration (~100-

300ms). The Nyquist ghosts can be distinguished from motion induced ghosting described above by the periodic shift of ghosts across the field of view. In addition, the Nyquist ghosts have the same intensity for each ghost, which is not normally true in motion-induced ghosts.

Origins/Causes: The method of k-space sampling in fast imaging techniques such as EPI where all signal echoes are acquired in one segment, or "shot", uses a very high bandwidth, enabling accelerated data collection. Once each line of k-space is acquired, frequency-encode gradients are quickly (and equally) reversed. This rapid gradient switching is coupled with a defined increment in the phase encode gradient, resulting in a "zig-zag" trajectory through k-space, with every other echo signal measured with a reversed gradient polarity. The general assumption is that each echo is perfectly phase-centered for each gradient-reversal step. However, gradients cannot achieve instantaneous gradient reversal, even with maximum slew rates, but, rather, finite time is required for gradient ramp up/down. These slight timing delays explain the notion of the so-called "zig-zag" k-space trajectory, and may cause an additional phase in the measured signal. The high demands placed on balanced timing delays and consistent gradient reversals make EPI susceptible to phase offsets propagated throughout k-space. When there is a fixed phase offset between each adjacent echo measurement, the Fourier transform of raw data into image space results in an object displacement of half the FOV. This displacement is akin to those discussed with respiratory artifacts: if each phase-encode step acquired data alternatively between inspiration and expiration, ghost artifacts would resemble those associated with Nyquist EPI ghosts.

Most systems are well-calibrated and do not experience any inherent gradient timing delays (even though ramp-up, ramp-down times always exist). But the unique k-sampling of EPI methods make it susceptible to other factors that may introduce unpredictable signal phase shifts. Essentially, any B_0 inhomogeneity will have an influence on consistent spatial localization. However, the most common cause is eddy currents in the gradient coils. These additional currents are induced in response to the rapidly switching gradients during EPI acquisitions. In effect, eddy currents produce an additional local gradient magnetic field, which is then superimposed onto the prescribed acquisition gradients.

Strategies for Alleviating Artifacts: As an initial step, Nyquist ghosts can be mitigated by addressing the factors impairing field homogeneity. It is important to use higher-order, advanced shim settings to reduce local inhomogenities. However, the likely culprits of Nyquist ghosts, in the absence of patient motion, are the consequences resulting from the high gradient demands of EPI, such as eddy currents and other unforeseen timing delays. While some system architecture exists for eddy current compensation, it benefits to identify this root cause. The isolation of gradient-related Nyquist ghosts can be

accomplished through re-calibration by a service engineer, or replicated through local phantom testing. With an MR phantom, field homogeneity and object motion can be controlled during EPI scanning. Moreover, other rapid sequences, such as signal-shot TSE, which also demand consistent, phase-centered echoes, can also be tested to reveal evidence of residual gradient mis-timing effects. It is possible to reduce the demands to the gradient system by lowering the gradient strength and switching speed. However, this may introduce other artifacts in place of Nyquists ghosts, such as distortion due to reduced phase-encode sampling rate. Ultimately, routine system service by an engineer may be needed to confirm findings and recalibrate gradients.

Another factor that lessens the likelihood for Nyquist ghosts are mechanisms that reduce the sequence echo train length (ETL). As alluded earlier in this section, increasing the number of k-space "segments" reduces the propagation of phase errors over the complete data set. Though ghosts may persist if evident system timing imperfections are present, the N/2-appearance may not obscure image quality as significantly. Other methods to reduce ETL include reducing the phase resolution (less N_y points) or utilizing parallel imaging.

3.2. CHEMICAL SHIFT ARTIFACTS

Appearance: Two variations of the chemical shift artifact manifest in MRI. A type 1 chemical shift artifact typically occurs in the frequency encode (k_x) direction, and is the product of spatial misregistration between fat and water protons. The appearance is dark etching along boundaries between fat and other tissues. This artifact is sometime referred to as the 'india-ink' artifact, as tissues appear to be outlined in dark ink, *figure 3*. In echo-planar imaging (EPI), such fat misregistration typically occurs in the phase-encode direction, and is commonly visualized when fat suppression is not used or is inhomogeneous. A type 2 chemical shift artifact occurs in all directions and within tissue itself. It presents as complete signal loss at as tissue signal loss dependent on the proportion of fat/water voxel composition, *figure 4*. Type 2 chemical shift artifact is commonly associated with gradient echo techniques, and is often viewed as beneficial for assessing diffuse fatty tissues, such as liver, or identifying fat containing lesions.

Origins/Causes: The basis of chemical shift artifacts is the difference in precession frequency between fat and water protons (3.5ppm). At 1.5T, this difference (Δf) translates to an offset of 220Hz, while at 3T, the difference is 440 Hz. This distinction allows the precise estimation of the fat/water mis-registration in the image: given field-of-view (FOV), bandwidth (BW_{read}), and matrix size (N_x), one can calculate the spatial water-fat shift (WFS):

$$WFS = \frac{FOV \cdot \Delta f}{N_x \cdot BW_{read}}$$

If the WFS is greater than the spatial resolution in the frequency encode direction, some fat components will superimpose onto neighboring pixels, revealing dark boundary effects. This is the typical feature of type 1 chemical shift artifact. The misregistration is exacerbated at high field strength given equivalent parameters, due to increased Δf. It is also evident when matrix and/or bandwidth are low, or FOV is large. The prevalence of type 1 artifact to the frequency encode direction (for non-EPI sequences) is due to the relatively low readout BW of these sequences, as well as the fact that transverse magnetization is either refocused or spoiled for each echo measurement. This effectively negates the accumulation of precession-related offsets in the phase-encode direction.

Precession differences are also the source of type 2 artifact, which is mainly associated with gradient echo imaging. If fat and water protons coexist in one voxel, they will become progressively out-of-phase relative to each other following RF excitation (3). If the pulse sequence is precisely timed, there will be a particular time in which fat and water protons are 180 degrees out-of-phase, resulting in signal cancellation. At 1.5T, this time occurs approximately every 4.4ms, beginning with 2.2ms. At 3T it occurs every 2.2ms, beginning with 1.1ms. Some gradient-echo sequences are timed such that the echo time (TE) occurs when fat and water are opposed-phase, so that important information about fat containing lesions and tissues can be observed. Typical applications also include an "in-phase" acquisition, in which a second echo is measured when fat and water are coherent. It is important to note that signal loss due to opposed-phase effects is proportional to the fractional content of fat in the voxel, with 50% resulting is complete signal loss. However, if the fractional content is greater than 50%, signal amplitude will increase, with fat protons predominating voxel concentration. It is also important to note that type 2 chemical shift signal loss does not naturally occur in spin echo imaging. This is due to 180 degree RF refocusing, with TE selected to coincide with complete re-phasing of transverse magnetization.

Strategies for Alleviating Artifacts: From the equation above, type 1 chemical shift artifact can be corrected by selecting imaging parameters appropriately. Since FOV and matrix are often fixed due to application criteria, increasing bandwidth often remedies the artifact. This tactic also has less SNR penalty than increases in image resolution. Alternatively, frequency and phase directions can be swapped, in lieu of any parameter adjustment, as long as other artifacts, such as aliasing and motion, are not adversely affected. One must also be wary of chemical shift at high field strengths, since one-to-one transfer of imaging parameters will not be optimal; a proportional increase in BW is necessary to achieve the same WFS as lower field strength. Another solution to eliminate the appearance of fat shifts is to employ fat saturation. Though effective, this clearly alters the imaging

application, and may not be warranted in clinical application.

As mentioned above, type 2 chemical shift artifact is often desired in many clinical applications. However, it is usually common to acquire a corresponding in-phase image concurrently. Since other factors, such as iron deposition or susceptibility, may also contribute to signal loss on gradient echo images, it is recommended to acquire opposed-phase images using the first out-of-phase TE (1.5T: 2.2ms; 3T: 1.1ms). In other applications that do not call for interrogating fat composition, elimination of the type 2 artifact is achieved simply by acquiring data using in-phase TEs (1.5T: 4.4ms; 3T: 2.2ms), or using fat suppression. Note that incomplete fat suppression may still result in type 2-related signal loss, if TE is chosen near the opposed-phase TE.

3.3. SUSCEPTIBILITY-RELATED SIGNAL LOSS

Appearance: Areas of local signal loss, signal pile up (non-anatomical bright and dark areas near each other), and warping of geometry.

Origin/Causes: When external magnetic fields are applied to tissues, the tissues alter the applied magnetic field based on their physical and chemical composition. Magnetic susceptibility is a property that indicates how magnetization is effected in a tissue in response to applied magnetic field. Tissues that strengthen the applied magnetic field, are called *paramagnetic* and substances weaken the applied magnetic field are *diamagnetic*. When adjacent tissues have large differences in magnetic susceptibilities, they produce changes in the magnetic field, so the *local* magnetic field is then altered from its expected value. This can cause complete signal loss at the interface if the frequency change causes the signal to become far off from the resonance frequency. It also causes changes in the frequency distribution during frequency encoding, leading to mis-mapping of signal position in the images. The mis-mapping can cause signal 'pile-up' where signal from different locations are assigned to the same position due to incorrect frequency position, *figure 5*. The local alterations in the field induces a gradient in the field which increases signal dephasing. This accelerates the T2-decay of the signal and is often called T2* to differentiate it from conventional T2 effects.

The size of the susceptibility artifact is proportional to:

$$Degree\ of\ suscept\ artifact \propto \frac{(\Delta\chi) \cdot TE \cdot B_0}{BW_{read}}$$

Where $\Delta\chi$ is the susceptibility, TE is the echo time, B_0 is the magnetic field strength and BW_{read} is the readouts (frequency) bandwidth (4, 5).

Location: Susceptibility artifacts are present in areas where there is a large natural susceptibility ($\Delta\chi$) difference between two adjacent tissues. The most common location for these artifacts to occur is at tissue-air interfaces, including near the lung, in the nasal sinuses, or at the body surface. Areas in the brain or liver that may have a large iron buildup due to a pathologic state may also show susceptibility effects. Another other common location for susceptibility-induced artifacts is near any metal implants in or on the body. The metal is highly paramagnetic or even ferromagnetic, inducing large local changes in the magnetic field.

Susceptibility artifacts are most often present in gradient echo sequences, especially in gradient echo EPI sequences due to the large and rapidly changing magnetic field gradient applied in this sequences. Note that the use of the susceptibility effects to enhance tissue characterization has recently become an active area of research. S*usceptibility-weight imaging (SWI)* uses the effect of susceptibility to characterize tissue properties, and is especially useful for looking at iron content in the brain (5).

Strategies for Alleviating Artifacts: Susceptibility artifacts are ultimately due to dephasing of spins due to the presence of local magnetic field gradients. Ways to mitigate this dephasing include using a spin echo sequence instead of a gradient echo sequence. By examining the susceptibility equation, we can see that reducing the echo time or using an ultrashort TE sequence can reduce susceptibility artifacts. Increasing receiver bandwidth also reduces artifacts. Reducing pixel size can also reduce susceptibility by reducing the bandwidth per pixel in the image, but this comes at a signal-to-noise penalty. New MRI sequences which incorporate several of these susceptibility-reducing attributes have recently been developed by several MRI scanner manufacturers, especially for imaging in the present of metal implants for orthopedic applications (6). Finally, susceptibility induced artifacts are also proportional to the magnetic field strength, so they will be more pronounced at higher fields, such as 3.0 Tesla scanners (6) (7).

3.4. ALIASING/WRAPAROUND/FOLDOVER

Appearance: Objects from beyond the prescribed FOV are superimposed on the opposite side of the image in the phase-encoding direction.

Origins/Causes: The tissue that is outside the prescribed field of view (FOV) is still excited by the RF pulse and is subject to the applied magnetic field gradients. The phase encoding gradient imparts phase shifts of +/- 180° over this FOV in the phase encoding direction. Tissue that is outside the FOV will have a phase shift that is either >180° or < -180°. A phase shift of a signal is that is, for example, 181° is equivalent to a phase shift of -179° because of the cyclic nature of the MRI signal. Therefore signal outside of the FOV will be 'wrapped' to the other side of the image, *figure 6*. The frequency encoding direction is not affected by aliasing, as the frequencies above of beyond the receiver bandwidth are ignored.

Location: When the prescribed FOV is smaller than the object in PE direction, and coils are present that can detect signal from outside of the FOV, aliasing can occur.

Sometimes a small amount of aliasing in the image is tolerable if it can be easily identified, it does not interfere with the part of the image that is of concern clinically, and the region that is contains aliasing artifact can be seen in another imaging sequence.

Strategies for Alleviating Artifacts: The easiest way to remove the aliasing artifact is to increase the FOV. Of course increasing the FOV without increasing the number of phase encoding lines will reduce the image resolution, and increasing the number of phase encoding lines will increase the scan time. Saturation slabs can be placed over the area outside the chosen FOV to remove signal from the area that would normally wrap into the image. Additionally, the phase encoding direction can be aligned along the shortest dimension in the image to reduce the change of phase wrapping. Finally over-sampling in the phase encoding direction can be done. This is essentially acquiring (but not displaying) data in the phase encoding direction. Aliasing artifacts affect all types of MR sequences using Cartesian (line by line) acquisition of k-space. Aliasing in radial sequences is seen as noise and blurring.

3.5. RF NOISE/INTERFERENCE

Appearance: Zipper lines, checkerboards, or herringbone structures appearing in the image.

Origins/Causes: The receiver coils are designed to pick up signals from the tissue in the body. This signal is quite small and therefore antennas need to be quite sensitive at detecting small amounts of RF. If there equipment that is putting off signal frequencies near the receiver coils, they will be picked up. This can be electronic equipment in the MRI room, or a leak in the copper Faraday cage that surrounds and shields the MRI scanner room. These spurious signals will be placed in k-space and transformed through the Fourier transform into image artifacts. The zipper pattern sometime seen along one direction in the image is related to noise arising at a specific frequency. The herring-bone patterns are usually related to a noise spike in k-space and may be related to poor coil connections or poorly performing coils, *figure 7*.

Strategies for Alleviating Artifacts: Ensure that there is no electronic equipment that is operating the MRI scanner room that is not specifically designed for operation in an MRI environment. Ensure that there are no new penetrations in the shielding surrounding the MRI scanner room. Analyze the door to MRI suite for leaks in the seal, and ensure the door is closed during scanning. Check coil connections and integrity of pins on the coils.

3.6. DIELECTRIC EFFECT

Appearance: Shading or focusing across the image, usually with the brightest or darkest area of the image near the center.

Origins/Causes: Resonant frequency is proportional to the strength of the main magnetic field. The wavelength of the transmitted RF pulse is inversely proportional to the resonant frequency so it decreases with increasing main magnetic field. At higher the magnetic fields (3.0 Telsa and above), the wavelength of the transmitted RF pulse in on the order of the dimension of the objects being imaged, causing the strength of RF field to vary with spatial position. The effect has been referred to as "field-focusing", because flip angles are increased or "focused" near the center of the field of view (8). However, the effects can be quite variable and are not easily predicted. These effects can generally be ignored at 1.5T, but must be considered at 3.0T and above.

Strategies for Alleviating Artifacts: The easiest way to remove the dielectric effect is to scan at a lower magnetic field strength (1.5 Tesla of below). A method to reduce variations in signal intensity at 3.0 Tesla is to use dielectric pads made with a high dielectric constant that reduces RF pulse inhomogeneity. Finally, use of specialized 'tailored' RF pulses can reduce the variation of the flip angle across the FOV (9).

3.7. TRUNCATION ARTIFACT/GIBBS RINGING

Appearance: The truncation artifact is also known as *Gibbs ringing*. As the name implies, the artifact manifests as faint lines propagating from tissues edges, especially sharp edges between high contrast tissues, *figure 8*. Additionally, truncation artifact tends to fade away rapidly. This latter appearance distinguishes it from motion-related artifact, which present as distinct replicas of the object. Moreover, even subtle motion artifacts, which present small ghosts or blurred edges, can be differentiated from truncation artifact, since they often affect all tissue objects diffusely. Truncation artifact is specific to sharp transition edges, and may not affect all tissues in the FOV. Finally, truncation artifact appears mostly with lower resolution images, which may be an element of fast imaging techniques.

Origin/Causes: "Truncation" refers to the idea that k-space data is not continuous, but discretely sampled. This places a limit on the maximum encoded spatial frequency. From Fourier analysis, a sharp ("box-shaped") interface can only be approximated with an infinite number of frequency components. Since it is not possible in MR to sample an infinite number of spatial frequencies, finite frequency sampling limits the frequency components that can effectively describe the sharp edge. This translates to an overshoot and undershoot of sinusoidal signals in the vicinity of the interface, which gradually fade away. Moreover, if too few frequency components are used to approximate an interface, a false widening of that edge is presented. In terms of acquisition parameters, the maximum spatial frequency component (k_{max}) in both directions is defined by the product of the number of points (N_x and N_y), the gradient strength (G_x and G_y), and

sampling rate (dt). Therefore, for given bandwidth and gradient settings, the matrix in both the phase and frequency direction dictates the prevalence of truncation artifact. Since the phase resolution is typically lower, truncation artifact predominates in the phase encode direction.

Strategies for Alleviating Artifacts: The most commonly used solution for truncation artifacts are smoothing filters applied to k-space data prior to image reconstruction. An important tradeoff is image blurring, which may not be desirable in certain applications. If SNR is sufficient, resolution should be increased in the direction of ringing. This also includes the slice direction in 3D imaging, which is a commonly under-sampled for speed and improved SNR. Interpolation with zero-filling is often used to improve apparent resolution, but it does not concomitantly reduce truncation artifact, since it does not introduce new high spatial frequency data.

3.8. IMPROPER FAT SUPPRESSION

Appearance: Areas of high and low signal in regions of fat within the body when fat suppression is employed. One key advantage of a resonant frequency difference between water and fat protons is the ability to selectively *saturate* the magnetization of fat in MR images. Fat suppression has many applications, including eliminating confounding high signal from post-contrast T1 weighted imaging, and making edema and inflammation more conspicuous on T2-weighted imaging. A variety of methods exist for fat suppression, but the primary procedure is application of a chemical-shift sensitive RF excitation, centered on the resonant frequency of fat. In actuality, fat has up to six different resonant frequencies, with the most significant occurring at 1.3ppm, 2.1ppm, and 0.9ppm. For this reason, spectrally-selective RF pulses must also have a prescribed bandwidth, but must be limited to prevent intruding water resonance at 4.7ppm.

Ideal fat suppression should ensure uniform low signal intensity across the entire field-of-view, and among all slices, making the appearance of poor fat saturation clearly evident in most MR images. Poor fat suppression presents as regional elevation of fat signal intensity. It primarily occurs along the periphery of large field-of-view images, and in areas of complex or abnormal tissue geometry, such as the abdomen, neck, or breast, *figure 9*. Fat suppression is also rendered ineffective around metal implants, or significant gas/air interfaces. Moreover, large axial slice coverage, as in abdominal imaging, may suffer from non-uniform fat suppression on more superior and inferior slices.

Origins/Causes: The common theme among the locations of poor fat suppression is local field inhomogenity. In the majority of MR acquisitions, the frequency offset for fat suppression RF pulses are tuned based on global shimming procedures established before scanning begins. It does not subsequently adjust for field

inhomogeneities caused by local susceptibility changes. If certain voxels exist in regions of high susceptibility, such as adjacent to metal, the local resonant offset of fat will be more pronounced than predicted 1.3ppm, which is targeted by pre-tuned RF pulses. Sharp geometric transitions also cause voxels in this vicinity to possess resonant frequencies far different that default values. Additionally, local inhomogeneity may increase line broadening for fat resonances, which also may extend beyond the finite saturation bandwidth. All these instances cause the incomplete excitation of fat protons.

Separate from local susceptibility changes, large FOV imaging also causes regions of poor fat suppression, primarily along the periphery of the FOV. Fat –containing voxels located along the periphery are significantly far from isocenter, where field inhomogeneity also predominates. This also pertains to multi-slice axial imaging; poor fat suppression is often seen on first and last slices of axial data sets with large number of slices.

Another source of poor fat suppression is inefficient spectrally-selective RF pulses. Two important factors affect these RF pulses. First, even though a finite excitation bandwidth is tuned to 1.3ppm, sharp frequency cutoffs are difficult to achieve, especially over a small spectral range. Consequently, the bell-shaped profile may cause some varying excitation of resonances inside and outside the frequency bounds. The second factor is the B1 field, which defines excitation efficiency of the fat saturation pulses. Similar to B0 inhomogeneity, perturbations in B1 field causes the RF excitation flip angle to be spatially variant. Hence, certain fat voxels may experience different saturation flip angles than other, which results non-uniform suppression. Typically, diaelectric effects, such as those experienced at high field strengths, significantly alter B1 field uniformity.

Strategies for Alleviating Artifacts: An immediate solution to poor fat suppression is improving the fat suppression pulses themselves. Using longer pulse durations with selective phase dispersion, or adiabatic RF excitation help improve the spectrum of targeted fat protons. Alternatively, spectral excitation can be performed on water protons only, whose spectral amplitude and line width are usually more well-defined than fat.

Since fat suppression methods are generally spectrally-selective RF pulses, converting to *short-tau inversion recovery (STIR)* techniques offers increased suppression uniformity over broad FOVs and field inhomogeneity. STIR utilizes a non-selective 180 degree inversion (IR) pre-pulse timed to null the longitudinal magnetization of fat protons prior to image acquisition. The longitudinal T1 recovery of fat is approximately 250ms at 1.5T, and is adequately nulled using an inversion time (TI) of 150 to 160ms. Since the IR pre-pulse affects both fat and water proton resonant frequencies, all tissue will undergo longitudinal T1 recovery. Most tissues relax slower than fat, and will not be suppressed at the selected TI; however, they will incur reduced available magnetization, which

translates to reduced image SNR. There will be similar tissue T1 relaxation with STIR post-contrast administration, restricting its use as a surrogate for fat-suppressed contrast-enhanced T1 imaging.

Another strategy for improved fat suppression uniformity is to perform manual shimming of the main (B0) magnetic field. This can be accomplished with locally-assigned shim volumes, or manually shifting the spectral location of fat saturation pulses. Since the former routine optimizes field homogeneity over a selected region, other locations in the field of view may suffer greater variance in fat suppression uniformity. In any scenario, it is useful to observe the spectral peaks of fat and water following any shimming procedure when fat suppression uniformity is desired. Even though broad line widths may still persist, manual frequency adjustments help to resolve significant fat frequency shifts caused by off-resonance. This strategy can be further optimized by using smaller field-of-views, or fewer slices, thereby limiting the effective volume of shimming.

More systems are now equipped with sophisticated fat-water separation techniques. These methods evolved from the well-known 2-point Dixon method, which exploits the known fat/water resonant frequency difference to generate separate fat-only and water-only images based on two time-shifted echo acquisitions. Modern Dixon methods still incur a scan time penalty, but are very efficient for creating robust fat-suppressed (water-only) images. These techniques do not rely on field-sensitive spectrally-selective pulses, or non-selective IR pulses, which reduce SNR of all tissues. However, the overall efficacy of the reconstruction is highly dependent on producing a suitable B0 field map. Nonetheless, unfavorable fat/water swapping can persist in regions of significant B0 field inhomogeneity.

4.0. RECONSTRUCTION RELATED ARTIFACTS

Appearance: Foldover or Aliasing artifacts that appears in the center of the field of view, hotspots in the images, lower signal to noise in the image.

Origins/Causes: The availability of parallel imaging methods has tremendously improved the utility of MR in a variety of applications (10). Parallel imaging involves utilizing multi-array receive coils over the imaged region, and using their individually-specific coil sensitivity to reconstruct under-sampled k-space data. Scan times can be reduced by 2 or more time with parallel imaging, but the side effect is reduced SNR and some associated artifacts. Typically, the reduction in SNR is tolerated in many applications that warrant fast acquisitions, especially if inherent SNR is high, such as is present in balanced SSFP in cardiac imaging. Often significant amplification of noise is seen with parallel imaging, when reduction factors exceed 3. Furthermore, if mulit-array coils are not properly placed around the region of interest, more noise

amplification is seen. These relationships are captured in a general equation for SNR in parallel imaging:

$$SNR \sim \frac{1}{g \cdot \sqrt{R}}$$

Where g is the geometric factor, related to interdependence of coil elements and placement, and R is the parallel imaging reduction factor, which represents to degree of k-space under-sampling (11).

Other associated parallel imaging artifacts derive from the reconstruction method. One parallel imaging method reconstructs undersampled k-space data using multiple coil sensitivity images in image space (e.g SENSE). Artifacts with this method appear similar to image foldover, although the aliased regions typically appear in the center of the field of view, and are sometimes mistaken as signal "hotspots", *figure 10*. Another common parallel imaging technique estimates missing imaging information in k-space (e.g. GRAPPA). If missing k-space data is not effectively recovered, unwanted phase shifts may develop, resulting in ghost-like artifacts in the phase encode direction.

Origins/Causes: As shown in the equation above, unwanted amplification of noise is due to increased parallel imaging factors, as well as poor coil design of placement. When selected phase encode data is skipped to achieve scan acceleration, the resultant image is an aliased version of the original object. Image-based parallel imaging techniques, like SENSE, rely on a pre-calibration of coil element sensitivities for image reconstruction. The coil sensitivity profiles from each element serve to estimate true (un-aliased) voxel signal intensity. If pre-calibration of coil sensitivities performs perfectly, this data can be estimated mathematically with high accuracy. However, several scenarios cause imperfections, such as poor coil sensitivity maps (due to faulty elements), poor coil placement (resulting in poor object signal profiles), or poor matching of calibration maps with actual object position (due to patient movement), cause inaccurate true image data computation.

For k-space-based parallel reconstruction, such as GRAPPA, missing phase encode lines are estimated for each coil using fully sampled reference lines called autocalibration signals (ACS) (12). The missing data from one coil element is estimated from ACS data from all other coil elements, and from the behavior of neighboring data lines. In this way, full k-space data is estimated for each coil element, prior to reconstruction. A final image is produced by combining the individual coil images. This iterative estimation process in k-space is sensitive to motion, so subtle phase ghosts may be exacerbated in the image. Moreover, poor coil geometry or placement may cause incomplete estimation of individual coil images, resulting in exaggerated noise bands in areas of poor coil coverage.

Strategies for Alleviating Artifacts: One must first identify whether poor SNR, ghosts, or aliasing are a result of parallel imaging, or other physiological or technical factors. One may also exchange parallel imaging techniques to see if artifacts are resolved. Separate from removing parallel imaging altogether, some strategies are available to optimize the use of SENSE or GRAPPA methods. Proper coil placement is a significant cause of parallel imaging artifact, so care must be taken to first set up coil coverage that is favorable for parallel imaging. This means ensuring adequate multi-array coils in the phase encode direction, which is non-trivial when flexible multi-array coils are used for extremity imaging. Furthermore, spine imaging often only uses posterior multi-array coils. This configuration favors parallel imaging (i.e. phase encoding) only in the inferior-superior or left-right directions.

For image-based parallel imaging, an overly small FOV should not be used; some extended phase FOV will alleviate subtle unfolding reconstruction artifact. Furthermore, effort should be made to match the anatomic positioning between coil calibration scans and pulse sequences using parallel imaging. This may require calibration scans to be performed using similar breath hold instructions.

K-space-based parallel uses auto-calibration steps built into the acquisition, so parallel imaging ghosts are usually rare. However, the technique is more sensitive to patient motion, or inadequate reference coil sensitivities. Often, more auto-calibration reference lines are needed, which reduces the scan acceleration. Increased reference lines also alleviate central noise banding, which is common with parallel imaging.

Finally, users must be wary of malfunctioning elements on multi-array coils. Clearly, this will affect overall image SNR, but even slightly underperforming coil sensitivity profiles will accentuate artifacts on sequences using parallel imaging. Routine system and coil maintenance is vital for optimal performance of sequences using parallel imaging.

5.0. MR PHYSICIST'S ROLE: QUALITY ASSURANCE AND CLINICAL SERVICE

As discussed in the preceding sections, MR artifacts regularly degrade routine clinical imaging in a variety of ways. It is also evident that many image abnormalities can be readily identified and corrected. Even though general guidelines to avoid artifacts should be communicated to MR technologists, it is not often possible to address all artifacts as they happen, especially system-related artifacts across multiple MR systems. Therefore, strategies and programs must be developed by MRI physicists to periodically monitor and analyze system performance prospectively. Through proactive system assessment, an MR physicist can be best prepared for addressing issues

before they occur, and discussing the outstanding needs to achieve a high quality diagnostic practice.

Though each MR system should have an established agreement with a vendor (or third-party) service engineer for preventative maintenance, overall system performance must be carefully evaluated and documented by an MR physicist. This begins with assessing the imaging capability of the MR system itself, which includes its basic system specifications (field and gradient strength, slew rate, effective field-of-view, etc.), as well as its array of imaging software applications (pulse sequence licenses, coil inventory, reconstruction options, etc.). From this survey, the physicist will have a better understanding of the limits of the system, thereby preventing subpar image quality, undesirable artifacts, or even unsatisfactory diagnostic results. This knowledge must be shared and discussed with all invested personnel, such as radiologists, technologists, and administration, but also used as ongoing insight into optimization strategies. This forms the primary goal of MR system hardware and software assessment: *to devise and implement optimized MR imaging protocols for clinical practice, with ongoing oversight and education of image quality and system performance.*

It is clear that the MR physicist's role is a balance between ensuring stable system performance and overseeing the varied aspects clinical MR operations. The specific division of these two roles may vary depending on the needs of the institution or involvement of other personnel in these areas. As mentioned, however, the essential duty is proactive system performance assessment. Beyond tabulating reports generated by service engineers and performing trend analyses, a comprehensive annual system performance evaluation should be performed to document baseline values for a variety of imaging metrics, such as geometric accuracy, contrast resolution, field and signal uniformity, slice thickness accuracy, and soft copy displays. Moreover, each system RF coil should be evaluated for signal-to-noise and signal uniformity, with deficiencies documented and relayed to appropriate service engineers. Importantly, this annual assessment will act as certification for local commission requirements for hospitals. There are ample resources available to assist in formulating and conducting an annual performance review, with the American College of Radiology (ACR) being the primary entity governing quality and accreditation in the United States. The ACR also provides guidelines and a multi-faceted MRI phantom, which facilitates performance testing. Recent changes to the ACR guidelines also call for a comprehensive assessment of the institution's MRI safety program, which should be conducted with delegated technologists, radiologists, and administrative leaders.

An MR physicist should also establish a weekly quality control program in partnership with MRI supervisors. Several guidelines exist regarding this effort, but essential tasks entail basic inventory and system visual checks by MRI staff, and limited phantom scanning to assess key performance metrics, such as geometric accuracy and low

contrast detectability. The MR physicist should oversee these weekly duties, monitor trends, and create action limits for deficiencies. The MR physicist should be also active in clinical MR operations. An important aspect of a proactive quality assurance in clinical MRI is the development and disseminating of MR educational materials for MRI staff. This involves establishing best practice MR protocols that limit the occurrence of MR artifacts with minimal technologist intervention. Examples of this effort include pre-programming appropriate FOVs, slice coverage, image contrast, image resolution, bandwidth, coil shimming, and motion compensation strategies into every protocol and sequence. In addition, the MR physicist should communicate these best practice imaging guidelines to MR staff to ensure compliance with protocols, while acting as an expert resource for feedback. This step is vital for revisiting protocols that are suboptimal. Similarly, an MR physicist should work in tandem with radiologists to translate clinical needs into MRI protocols, while suggesting appropriate imaging options based on the capabilities of the MR system. These important relationships with both MRI staff and radiologists are mutual feedback loops, with the overriding goal to efficiently achieve optimal diagnostic image quality on a routine basis.

The knowledge of an MR system's hardware and software capabilities plays an important role in an MR physicist's relationship with administrative leaders. Growth, innovation, and new imaging services in a department depend largely on updating or procuring new MR systems. It is important for MR physicists to engage themselves with administration and serve as expert advisors throughout the process of system purchase or modifications, including site planning, safety assessment, and system technical configurations.

REFERENCES

1. Brown R, Cheng, Y., Haacke, E., Thompson, M., & Venkatesan, R. Magnetic Resonance Imaging Physical Properties and Sequence Design (2nd ed.) ed. Hoboken: Wiley; 2014.

2. Feng L, Benkert T, Block KT, Sodickson DK, Otazo R, Chandarana H. Compressed sensing for body MRI. J Magn Reson Imaging. 2017;45(4):966-87. doi: 10.1002/jmri.25547. PubMed PMID: 27981664; PMCID: PMC5352490.

3. Dixon WT. Simple proton spectroscopic imaging. Radiology. 1984;153(1):189-94. doi: 10.1148/radiology.153.1.6089263. PubMed PMID: 6089263.

4. Schenck JF. The role of magnetic susceptibility in magnetic resonance imaging: MRI magnetic compatibility of the first and second kinds. Med Phys. 1996;23(6):815-50. doi: 10.1118/1.597854. PubMed PMID: 8798169.

5. Qiu D, Chan GC, Chu J, Chan Q, Ha SY, Moseley ME, Khong PL. MR quantitative susceptibility imaging for the evaluation of iron loading in the brains of patients with beta-thalassemia major. AJNR Am J Neuroradiol. 2014;35(6):1085-90. doi: 10.3174/ajnr.A3849. PubMed PMID: 24578278.

6. Hargreaves BA, Worters PW, Pauly KB, Pauly JM, Koch KM, Gold GE. Metal-induced artifacts in MRI. AJR American journal of roentgenology. 2011;197(3):547-55. doi: 10.2214/AJR.11.7364. PubMed PMID:21862795.

7. Oshinski JN, Delfino JG, Sharma P, Gharib AM, Pettigrew RI. Cardiovascular magnetic resonance at 3.0 T: current state of the art. J Cardiovasc Magn Reson. 2010;12:55. doi: 10.1186/1532-429X-12-55. PubMed PMID: 20929538; PMCID: PMC2964699.

8. Hoult DI, Phil D. Sensitivity and power deposition in a high-field imaging experiment. J Magn Reson Imaging. 2000;12(1):46-67. PubMed PMID: 10931564.

9. Sung K, Nayak KS. Design and use of tailored hard-pulse trains for uniformed saturation of myocardium at 3 Tesla. Magnetic resonance in medicine : official journal of the Society of Magnetic Resonance in Medicine / Society of Magnetic Resonance in Medicine. 2008;60(4):997-1002. doi: 10.1002/mrm.21765. PubMed PMID: 18816833.

10. Blaimer M, Heim M, Neumann D, Jakob PM, Kannengiesser S, Breuer FA. Comparison of phase-constrained parallel MRI approaches: Analogies and differences. Magnetic resonance in medicine : official journal of the Society of Magnetic Resonance in Medicine / Society of Magnetic Resonance in Medicine. 2016;75(3):1086-99. doi: 10.1002/mrm.25685. PubMed PMID: 25845973.

11. Pruessmann KP, Weiger M, Scheidegger MB, Boesiger P. SENSE: sensitivity encoding for fast MRI. Magnetic resonance in medicine : official journal of the Society of Magnetic Resonance in Medicine / Society of Magnetic Resonance in Medicine. 1999;42(5):952-62. PubMed PMID: 10542355.

12. Griswold MA, Jakob PM, Heidemann RM, Nittka M, Jellus V, Wang J, Kiefer B, Haase A. Generalized autocalibrating partially parallel acquisitions (GRAPPA). Magnetic resonance in medicine : official journal of the Society of Magnetic Resonance in Medicine / Society of Magnetic Resonance in Medicine. 2002;47(6):1202-10. doi: 10.1002/mrm.10171. PubMed PMID: 12111967.

Contact:
Phone: 404-727-5894
Email: jnoshin@emory.edu
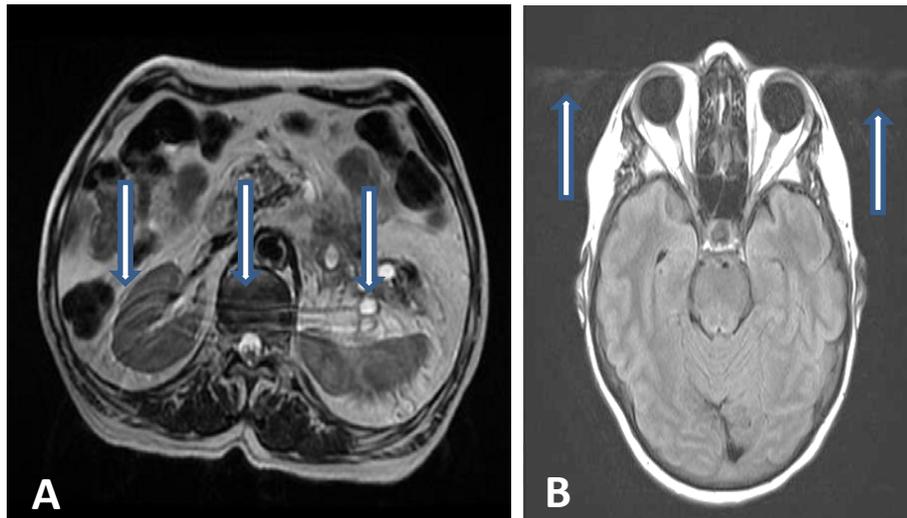
Figure 1. Motion and Phase Encoding Artifacts. Motion between phase encoding steps causes tissue to see different gradient strengths throughout the imaging process causing non-reproducible phase shifts between k-space lines. The results of this after the Fourier transform is misplacement of tissue related to the periodicity and extent of motion. This is most commonly seen as 'ghosting' of bright tissue such as vessels or fat in the phase encoding direction of the image. A) Respiratory ghosts on Axial T2 TSE; B) Non-periodic ghosts from eye movements on Axial T2 FLAIR.
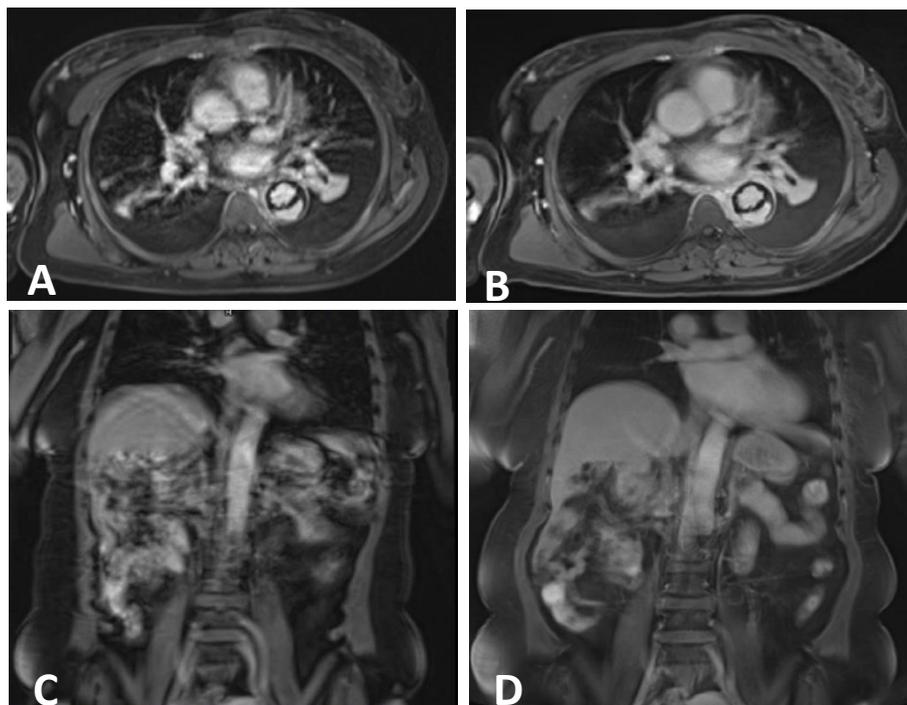
Figure 2. Motion and Respiratory Compensation. Poor breath holding may cause motion ghosts and/or blurring (A, C). Radial k-space sampling is an effective way to lessen the appearance of high signal ghost propagation by oversampling the center of k-space. Longer scan times are required to adequately sample the periphery of k-space to recapture image detail (B, D)
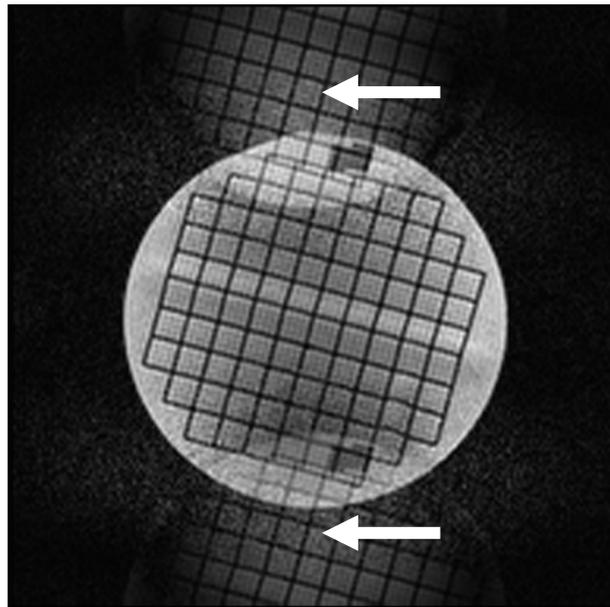
Figure 2. Nyquist Ghosting. Nyquist ghosting are artifacts appear as distinct copies of the imaged object, propagated across the FOV in the phase encode direction in EPI or other fast imaging techniques. They are related to a phase shift acquired during rapid gradient switching in accelerated imaging techniques. The White Arrow show the Nyquist ghosts.
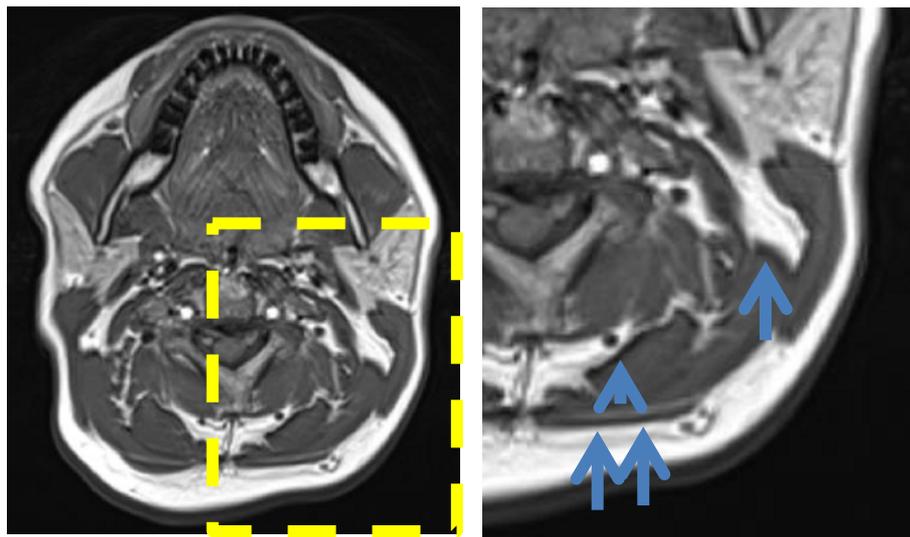

Figure 3. Chemical Shift Artifacts – Type 1. Chemical shift artifact of the first kind is caused by fat and water having slightly different procession frequencies. If the imaging bandwidth is too low, these differences in frequencies can cause a displacement in the location of fat relative to other tissues in the image space. The result is a black line (blue arrows) at the interface of fat and water where the displacement occurs. (see inset) For spin echo, chemical shift occurs in the frequency encode direction, while for echo-planar, it occurs in the phase encode direction
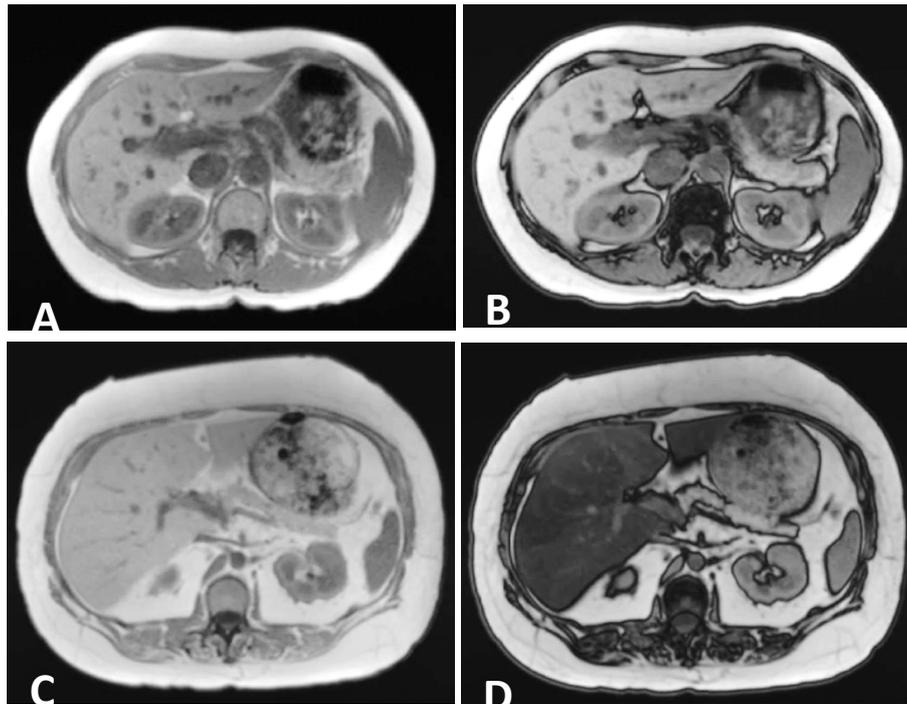
Figure 4. Chemical Shift Artifacts – Type 2. Chemical shift artifact of the second kind is also caused by fat and water having slightly different procession frequencies. At certain echo times the fat and water can be in-phase and other echo times they can be out of phase. When voxels contain both water and fat, in-phase images will add together to increase signal in a voxel (A, C). When fat and water are out of phase, fat and water will cancel each other and reduce signal along fat-water interfaces(B, D). When a subject has fatty liver disease., liver signal is reduced, proportional to the fat percentage (D).
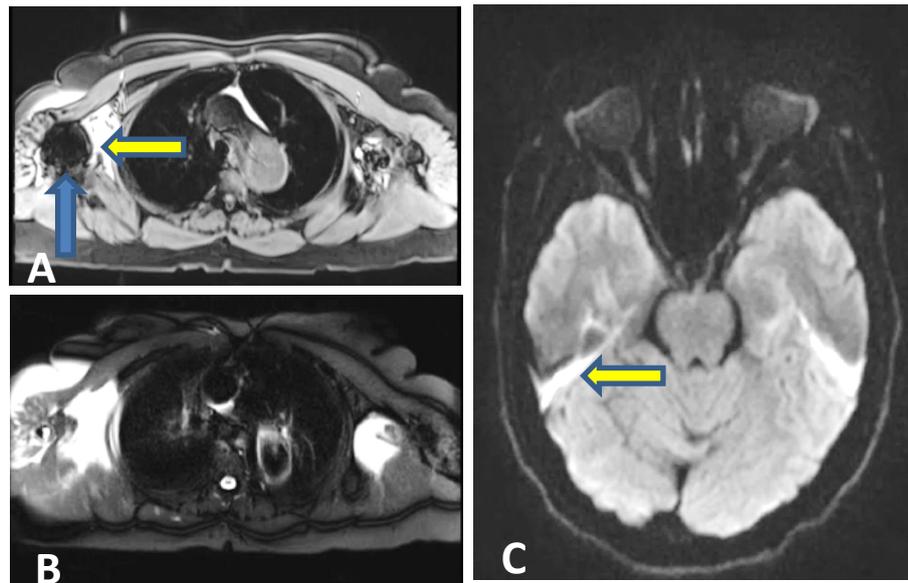
Figure 5. Susceptibility-Related Signal Loss and Signal Pile-up. When adjacent tissues have different magnetic properties or magnetic susceptibility, the *local* magnetic field is altered from its expected value, leading to signal mis-mapping in the images, or signal 'pile-up' (yellow arrow). It can also lead to local alterations in the field which change the signal from the resonant condition resulting in complete signal loss (blue arrow). A) This artifact was due to a metal implant, and is significant on gradient-echo imaging; B) Signal loss/distortion is reduced using TSE; however fat-sat is non-uniform around significant inhomogeneity. C) signal distortion pile-up on DWI due to air-tissue susceptibility interface
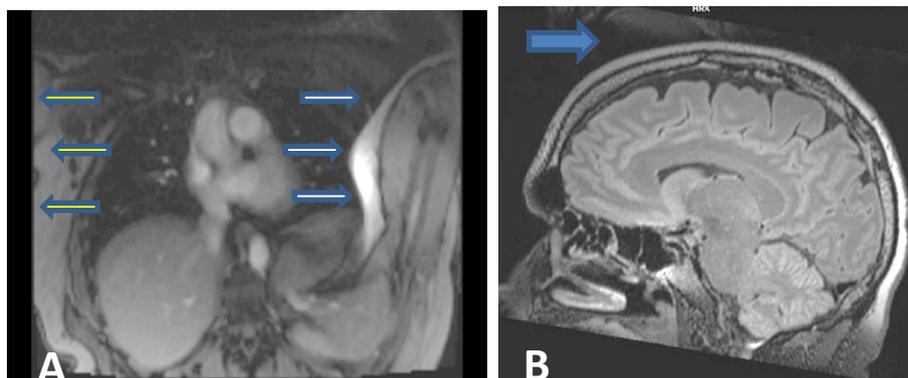

Figure 6. Aliasing / Wraparound / Foldover Artifact. The artifact occurs when tissue outside of the field of view receives the RF excitation pulse and generates a signal which is outside the readout bandwidth. The results is tissue 'wrapping around' to the other side of the image in the phase encoding direction. (A) The white arrows show the wrapped or aliased tissue and the yellow arrow show the edge of the prescribed FOV, which does not include the arm. Solution include increasing the FOV, using phase over-sampling, or pre-saturating tissue outside the FOV. B) On axial 3D imaging, aliasing may also occur in the slice direction, as seen on this sagittal reconstruction (blue arrow)
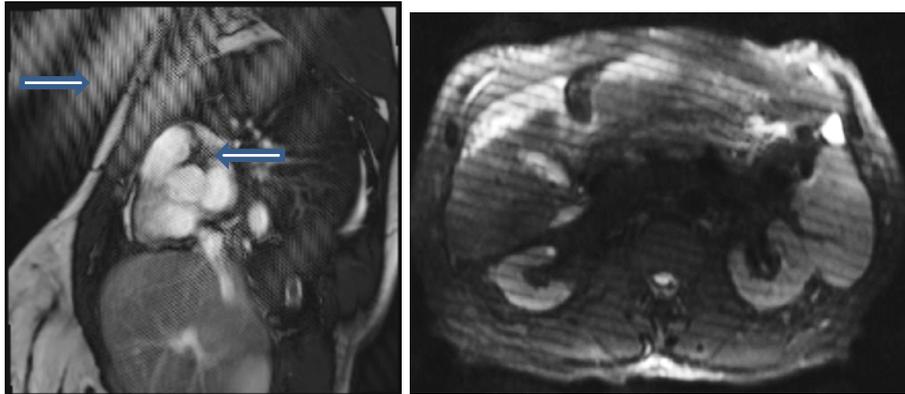
Figure 7. RF noise / Interference. If signals unrelated to the MR signal from tissue, but in the frequency range of the expected signal in the image, are present in the scanner room, they will be detected by the RF receiver coil. These noise signal will be put into k-space and transformed into the image. Because of the spatial frequency distribution of k-space, these signal will appears as 'zipper' or herringbone' artifacts.
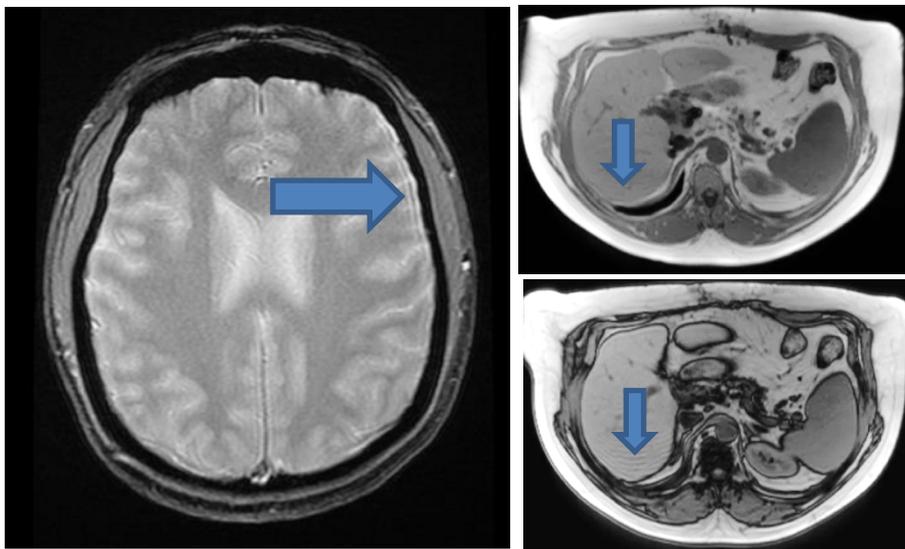

Figure 8. Truncation Artifact / Gibbs Ringing. Gibbs ringing is a result of truncating the acquisition of higher spatial frequencies in k-space. The lack of acquisition of high spatial frequencies causes edges in the image that have sharp boundaries in space and high signal intensity differences to appear to have a ringing effect. This is an artifact of the Fourier transforms being unable to represent a steep signal-step in image space. Ringing will evolve from high contrast edges if the resolution is low, which typically occurs in the phase encode direction, as in these examples (blue arrows).